Supporting Information for
The influence of hyporheic fluxes on regional groundwater discharge zones

Brian Babak Mojarrad[1], Anders Wörman[1], Joakim Riml[1], Shulan Xu[2]

[1]Department of Sustainable Development, Environmental Science and Engineering, KTH Royal Institute of Technology, Stockholm, 100 44, Sweden
[2]Xu Environmental Consulting AB, Stockholm, 168 61, Sweden

Correspondence to: Brian B. Mojarrad (mojarrad@kth.se)

Contents of this file

Figures S1 to S7

Tables S1 and S2

Introduction

This supporting information contains the study domain characteristics which were used in our analysis but not found in the main paper, including soil type map which was used in catchment-scale modeling, selected regions for rescaling to reflect the topography realiation in streambed scale modelling (Fig. S1), depth decaying function of streambed sediment hydraulic conductivity using Morén et al., (2017) experimental data (Fig. S2), considered subcatchments in streambed scale's dynamic head coefficient based on deep groundwater discharge points within the catchment (Fig. S3), schematic sketch showing the particle statistics of particle tracing results (Fig. S4), $\langle|W_S|\rangle$, in different parts of the study catchment (Fig. S5), cumulative distribution function of the ratio of the deep groundwater flow upwelling areas between the release surface and the bottom of the sediment layer (Fig. S6), flow transfer rate coefficient within the sediment layer (Fig. S7). Furthermore, the document includes stream flow properties for each streambed flow model used in dymaic head coefficient determination (Table S1), and Dynamic head coefficients for different topography realization and different stream characteristics (Table S2).

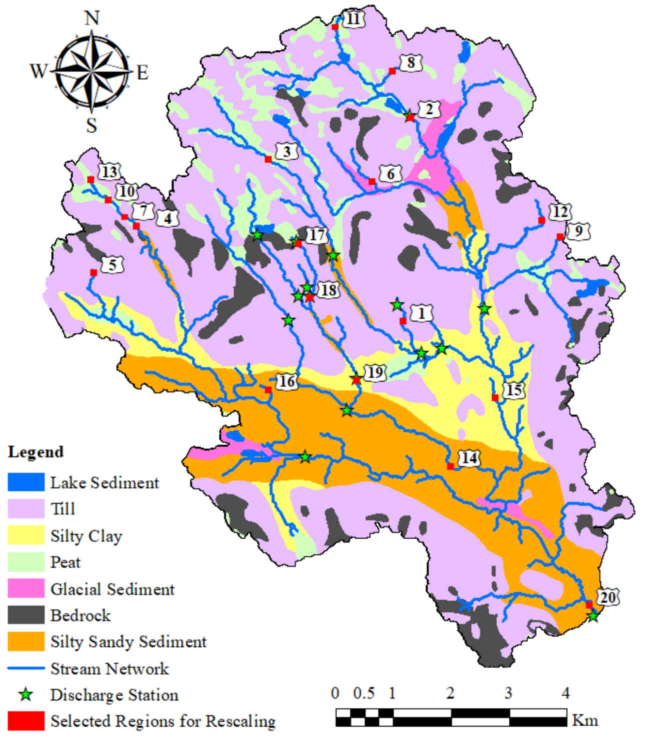

Figure S1. Map showing the soil type map of Krycklan catchment as well as stream network blue lines), and the discharge stations (green stars) within the catchment. Moreover, the position of the selected 100×100 m^2 regions for rescaling of the local streambed topography (red squares) used in the streambed-induced model are also shown. The labels correspond to selected 100×100 m^2 regions which were used as the topography realization in streambed scale modelling.

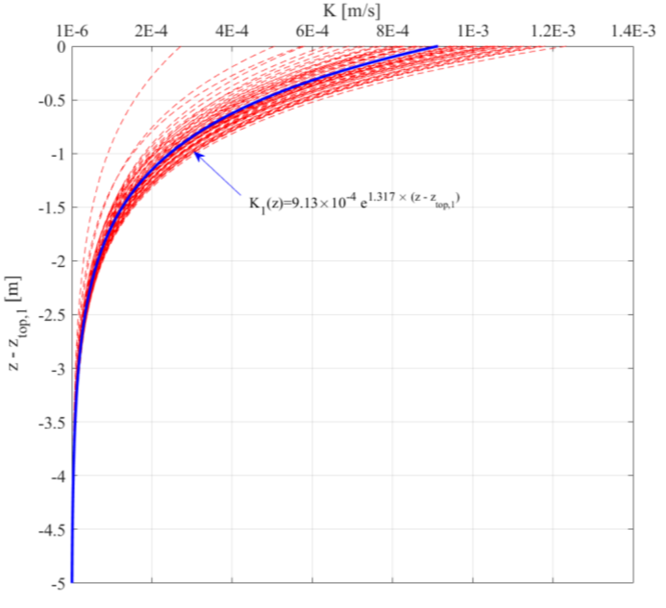

Figure S2. Depth decaying function of streambed sediment hydraulic conductivity using Morén et al., (2017) experimental data. They measured hydraulic conductivity of streambed sediment at two depths (i.e., 3 and 7 cm) with a spatial interval of 100 m for 5800 m of a small Swedish stream (Tullstorps Brook). The exponential function was fitted to each measured location with a lower hydraulic conductivity limit set to K= 10^{-6} (m/s) representing silty sandy sediment for the bottom surface of the streambed sediment layer (i.e., 5 m depth from the top surface). Red dashed lines represent the decay function for each measured point along the stream; blue solid line represents the decaying function using mean value of $K_{s,top}$ and mean of empirical decay coefficient ($1/\delta$) of all the measured points along the stream.

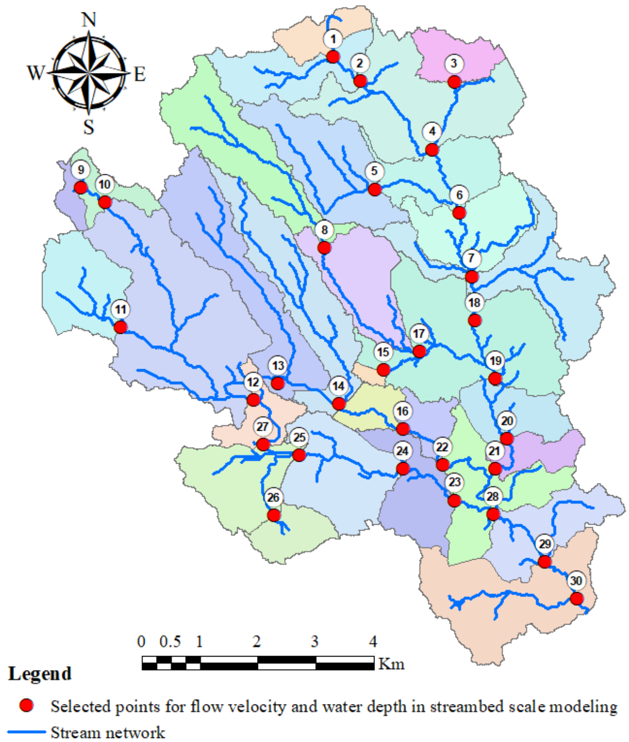

Figure S3. Map showing selected points for flow velocity (V_f) and water depth (D_w) used in streambed modelling (red point) as well as stream network (blue lines). In addition, the drainage subcatchment area for each point is shown in different color with a unique label.

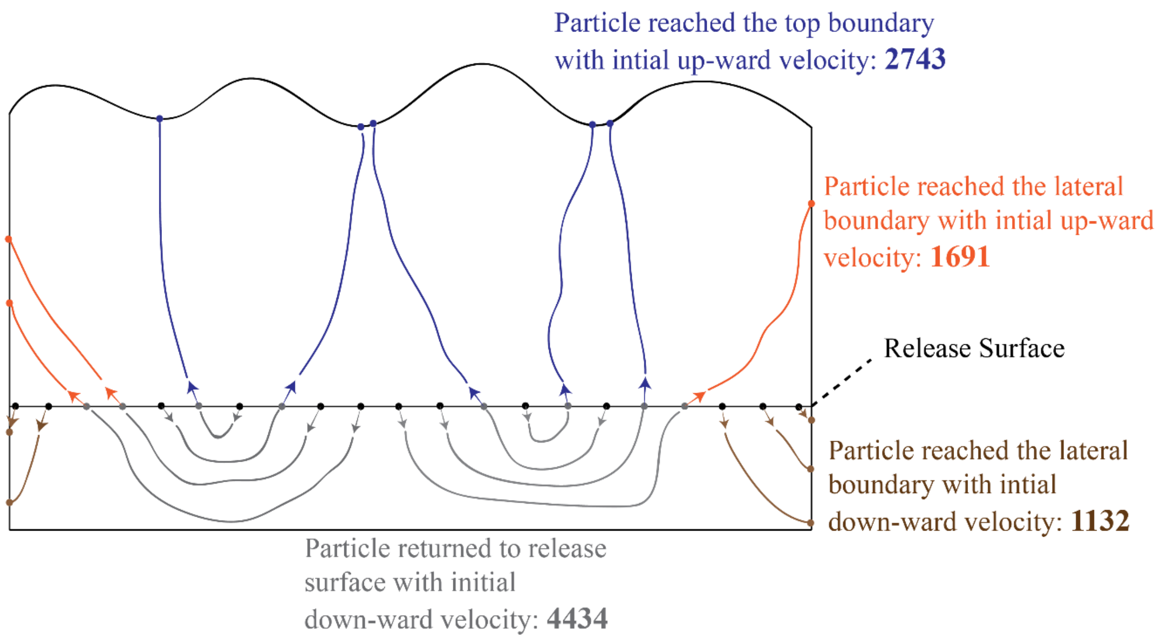

Figure S4. Schematic sketch showing the particle statistics of particle tracing results. Particles trajectory with initial negative vertical velocity is presented with grey and brown colours whereas, particle having initial positive vertical velocity are presented with blue and orange colours. Blue line shows the trajectories of the particle that ended op at the topography surface.

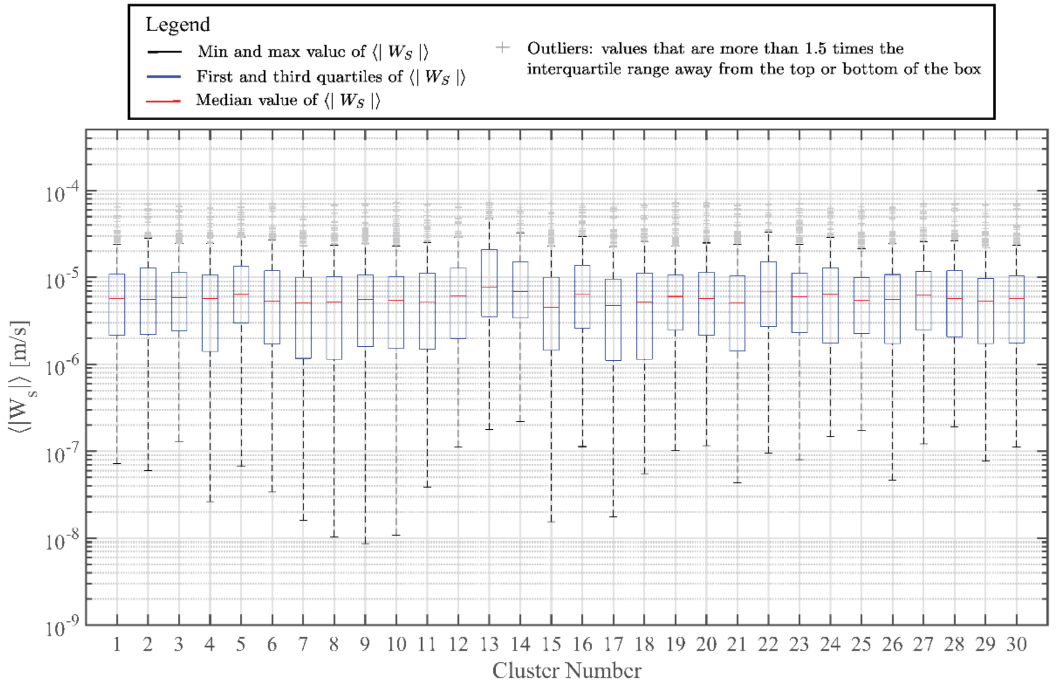

Figure S5. Mean value of the absolute value of the vertical velocity at the streambed interface of streambed scale flow, $\langle|W_S|\rangle$, in different parts of the study catchment (see Figure S3 in supporting information for the drainage area labels)

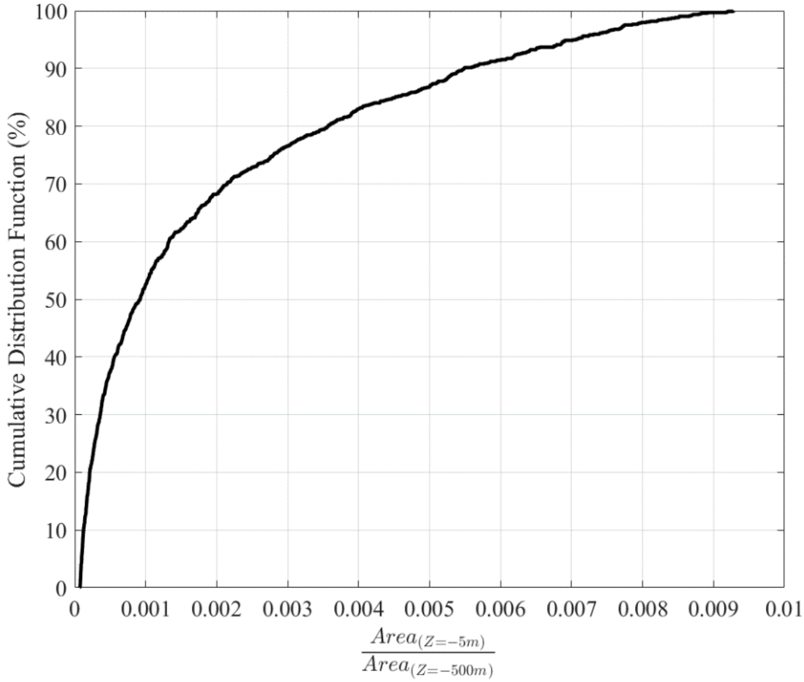

Figure S6. Cumulative distribution function of the ratio of the deep groundwater flow upwelling areas between the release surface and the bottom of the sediment layer evaluated using the continuity equation along the particle trajectories.

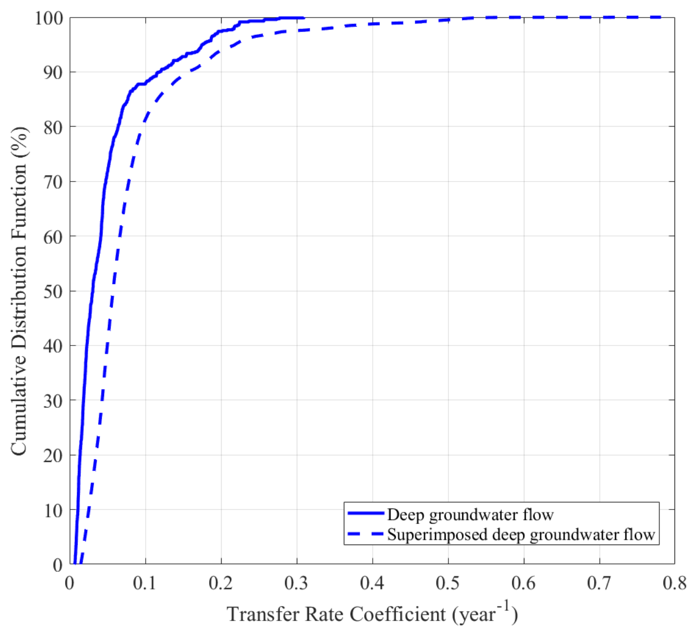

Figure S7. Cumulative distribution function plot of and deep groundwater flow transfer rate coefficient within the sediment layer (i.e., 5×5×5 m cubes); the solid line represent the catchment scale results (without the streambed induced flow influence), whereas the dashed line represent the superimposed results (catchment scale flow superimposed with the streambed scale induced flux).

Table S1. Stream flow properties for each streambed flow model

Drainage Area Label (from Figure S2)	Drainage Area (m^2)	Discharge (L/s)	Water Depth (m)	Mean Slope of the Stream Segment
1	887264	12.12	0.1298	0.0119
2	2863347	39.12	0.1247	0.0042
3	1039164	14.20	0.1175	0.0141
4	8442547	115.35	0.18	0.0115
5	3081226	42.10	0.0784	0.0042
6	13496213	184.4	0.28	0.0071
7	15739565	215.05	0.38	0.0120
8	3218440	38	0.41	0.0143
9	374543	3.42	0.18	0.0067
10	1125351	10.28	0.18	0.0079
11	2103602	19.22	0.18	0.0048
12	9659557	88.25	0.31	0.0044
13	3648469	34.60	0.0585	0.0341
14	7026528	66.64	0.1251	0.0011
15	147354	1.74	0.1056	0.0027
16	7757088	73.57	0.0781	0.0306
17	5441980	64.26	0.38	0.0241
18	19135916	261.46	0.25	0.0291
19	30099755	354.42	0.25	0.0056
20	31555891	371.57	0.25	0.0033
21	32414577	381.68	0.32	0.0043
22	8533691	80.93	0.0763	0.0099
23	18575299	169.71	0.4156	0.0071
24	16749702	153.03	0.3502	0.0049
25	13852445	126.56	0.31	0.0091
26	981744	8.97	0.0912	0.0128
27	10700797	97.77	0.31	0.0046
28	62053077	730.67	0.32	0.0039
29	64082749	754.57	0.38	0.0027
30	67937760	799.96	0.38	0.0016

Table S2. Dynamic head coefficients for different topography realization and different stream characteristics (refer to Figure S3 and Table S1)

Topography Sample / Drainage Area	Topo 1	Topo 2	Topo 3	Topo 4	Topo 5	Topo 6	Topo 7	Topo 8	Topo 9	Topo 10	Topo 11	Topo 12	Topo 13	Topo 14	Topo 15	Topo 16	Topo 17	Topo 18	Topo 19	Topo 20
NO. 1	0.037	0.057	0.036	0.036	0.068	0.095	0.034	0.044	0.051	0.038	0.035	0.035	0.056	0.036	0.039	0.194	0.039	0.083	0.072	0.054
NO. 2	0.042	0.065	0.039	0.041	0.079	0.105	0.039	0.051	0.059	0.042	0.038	0.038	0.064	0.042	0.043	0.214	0.043	0.091	0.082	0.063
NO. 3	0.052	0.081	0.045	0.051	0.097	0.121	0.048	0.062	0.073	0.049	0.044	0.044	0.079	0.051	0.050	0.246	0.049	0.105	0.101	0.077
NO. 4	0.012	0.018	0.016	0.012	0.022	0.044	0.013	0.014	0.016	0.018	0.016	0.016	0.018	0.012	0.018	0.089	0.018	0.038	0.023	0.017
NO. 5	0.062	0.096	0.048	0.060	0.115	0.091	0.057	0.074	0.087	0.045	0.049	0.049	0.094	0.061	0.044	0.186	0.045	0.079	0.121	0.092
NO. 6	0.002	0.002	0.003	0.002	0.003	0.008	0.002	0.002	0.002	0.003	0.003	0.003	0.002	0.002	0.003	0.015	0.003	0.007	0.003	0.002
NO. 7	0.006	0.009	0.006	0.005	0.010	0.017	0.005	0.007	0.008	0.007	0.006	0.006	0.008	0.005	0.007	0.035	0.007	0.015	0.011	0.008
NO. 8	0.003	0.004	0.005	0.004	0.005	0.013	0.004	0.003	0.004	0.005	0.005	0.005	0.004	0.003	0.005	0.026	0.005	0.011	0.005	0.004
NO. 9	0.000	0.001	0.000	0.000	0.001	0.001	0.000	0.000	0.000	0.001	0.000	0.000	0.001	0.000	0.001	0.003	0.001	0.001	0.001	0.001
NO. 10	0.003	0.005	0.004	0.003	0.006	0.012	0.003	0.004	0.004	0.005	0.004	0.004	0.005	0.003	0.005	0.024	0.005	0.010	0.006	0.005
NO. 11	0.015	0.023	0.021	0.015	0.027	0.055	0.016	0.018	0.021	0.022	0.020	0.020	0.022	0.015	0.023	0.112	0.022	0.048	0.029	0.022
NO. 12	0.038	0.032	0.053	0.040	0.038	0.141	0.042	0.031	0.029	0.057	0.051	0.051	0.031	0.039	0.059	0.288	0.058	0.123	0.040	0.030
NO. 13	0.308	0.476	0.237	0.298	0.572	0.325	0.284	0.369	0.430	0.224	0.244	0.243	0.464	0.302	0.219	0.663	0.222	0.282	0.599	0.455
NO. 14	0.022	0.033	0.020	0.021	0.040	0.053	0.020	0.026	0.030	0.022	0.019	0.019	0.032	0.021	0.022	0.109	0.022	0.046	0.042	0.032
NO. 15	0.004	0.006	0.003	0.004	0.007	0.008	0.003	0.004	0.005	0.003	0.003	0.003	0.006	0.004	0.003	0.015	0.003	0.007	0.007	0.005
NO. 16	0.082	0.126	0.063	0.079	0.152	0.119	0.075	0.098	0.114	0.059	0.065	0.064	0.123	0.080	0.058	0.243	0.059	0.104	0.159	0.121
NO. 17	0.007	0.004	0.009	0.007	0.005	0.024	0.007	0.005	0.004	0.010	0.009	0.009	0.004	0.007	0.010	0.049	0.010	0.021	0.005	0.004
NO. 18	0.022	0.024	0.031	0.023	0.028	0.083	0.025	0.018	0.021	0.033	0.030	0.030	0.023	0.023	0.034	0.169	0.034	0.072	0.030	0.023
NO. 19	0.041	0.043	0.057	0.043	0.052	0.152	0.046	0.034	0.039	0.061	0.055	0.055	0.042	0.042	0.063	0.310	0.062	0.132	0.055	0.042
NO. 20	0.045	0.048	0.063	0.047	0.057	0.167	0.050	0.037	0.043	0.067	0.061	0.061	0.047	0.046	0.069	0.341	0.068	0.145	0.060	0.046
NO. 21	0.022	0.017	0.030	0.022	0.021	0.079	0.024	0.017	0.016	0.032	0.029	0.029	0.017	0.022	0.033	0.162	0.032	0.069	0.022	0.016
NO. 22	0.121	0.188	0.093	0.118	0.226	0.173	0.112	0.145	0.170	0.089	0.096	0.096	0.183	0.119	0.087	0.353	0.088	0.150	0.236	0.180
NO. 23	0.039	0.023	0.055	0.041	0.028	0.145	0.043	0.031	0.026	0.058	0.053	0.053	0.024	0.040	0.060	0.295	0.059	0.126	0.029	0.024
NO. 24	0.059	0.043	0.082	0.061	0.051	0.218	0.065	0.047	0.039	0.088	0.079	0.079	0.042	0.060	0.090	0.444	0.089	0.189	0.054	0.041
NO. 25	0.079	0.065	0.109	0.082	0.078	0.291	0.087	0.063	0.059	0.117	0.105	0.106	0.064	0.081	0.121	0.593	0.119	0.253	0.082	0.062
NO. 26	0.033	0.052	0.026	0.032	0.062	0.058	0.031	0.040	0.047	0.024	0.026	0.026	0.050	0.033	0.024	0.118	0.024	0.050	0.065	0.049
NO. 27	0.047	0.039	0.065	0.049	0.047	0.173	0.052	0.038	0.035	0.070	0.063	0.063	0.038	0.048	0.072	0.354	0.071	0.151	0.049	0.037
NO. 28	0.079	0.063	0.110	0.082	0.076	0.291	0.087	0.063	0.057	0.117	0.106	0.106	0.061	0.081	0.121	0.594	0.119	0.253	0.079	0.060
NO. 29	0.039	0.026	0.054	0.040	0.031	0.143	0.043	0.031	0.026	0.058	0.052	0.052	0.025	0.040	0.059	0.292	0.059	0.125	0.032	0.024
NO. 30	0.044	0.029	0.061	0.045	0.035	0.161	0.048	0.035	0.029	0.065	0.058	0.059	0.028	0.045	0.067	0.329	0.066	0.140	0.036	0.027